Flow Induced Vibration of X-ray Optics

Zichen Xiao

Mentors: Dr. Curt Preissner and Jeffrey Collins

Abstract:

X-ray beams have a variety of uses in all scientific fields and the quality of those researches greatly depend on the brightness, stability and precision of the beam. Because x-ray beams can deposit a significant amount of power on the X-ray optics, liquid cooling, such as water or liquid nitrogen, is needed to cool the optics. However, the cooling flow can create unwanted vibration, which could largely affect the stability of the beam. Experiments and computer simulation were used to investigate different factors of flow-induced vibration of X-ray optics and compared standard hoses to a new type of lined hose. The lined hose was found to have lower pressure fluctuations above 300 Hz, which should correlate to lower vibration levels of the X-ray optic. However, lower vibration levels were not observed in the experiments as measured response was dominated by the fluctuating background vibration.

Introduction:

There are two main purposes for this study: First, investigate the effect of the lined hose on the vibration of the system; second, build a simulation model to gain insight into how X-ray optic systems vibrate and input to the model will be measured pressure fluctuations. The theory is well developed that coolant can cause the vibration of X-ray optics. [1] In this project, we are assuming that coolant pressure fluctuations will drive the vibration of the hose and the optic; [1, 2] simultaneously, the movement of the hose will affect the optics it connects with further more. In order to gain more understanding about flow-induced vibration situation, the vibration analysis will be tried to accomplish from two tracks: Hands-on measurement, including the hose and the optic, and computer simulation of the system. To simulate the real optics used in beamline, a set-up has been designed, including a single 6061 aluminum alloy block with metallic ports for transducers (representing the optic), a kinematic mounting structure, and a set of cooling connections. A fastener slot is designed in the middle of the block to apply the force to connect the block and plate. Foam is put under the plate to provide an easily quantifiable boundary condition.

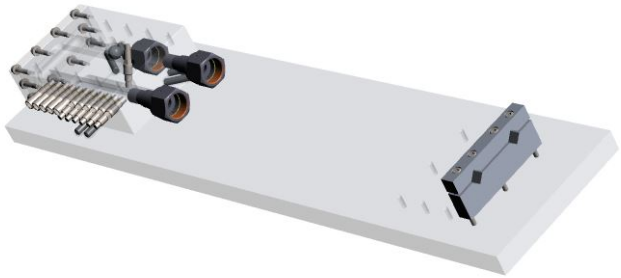

Figure 1(left) and 2 (right): Pictures of the designed and real experimental setup for measurement of pressure fluctuations and vibration (including transducers and catheter).

For the computer simulation, we first input the basic geometric CAD file of the system into ANSYS 14.5. The basic geometry was simplified and we excluded the connections, ports and other features that were not relevant or were not expect to affect our analysis. Then, for the sake of analysis convenience, we wanted to provide features for construction of the spring elements to replace mounting in the system. So Design Modeler, the geometry modeler in ANSYS was used to modify the original CAD file for analysis.

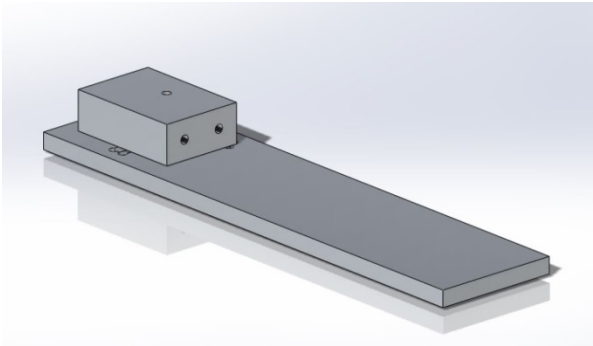

Figure 3: Original input geometry for ANSYS analysis

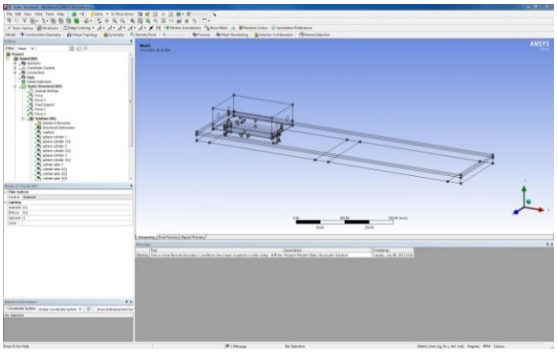

Figure 4: The interface of ANSYS Design Modeler shown as edges and vertices in this view

Methodology:

In the project, three pieces of data were measured: 1) the pressure drop across the test piece, 2) the fluid pressure fluctuations, and 3) the vibration of the table, base plate and optic. Because pressure fluctuations drive the vibration, it is useful to measure the pressure fluctuations at various points in the system. In addition, these data can be used as input to our simulation. To measure the pressure field, two methods had been designed: the first one was installing Piezo pressure transducers, PCB model S112A22 (S prefix means stainless steel diaphragm) in the tapped ports, which were specifically designed on the optic block. Those ports were 10mm away from each other and could investigate the channel wall pressure at those points. The second method was using a SPR-320 pressure catheter from Millar Instruments, which is commonly used to measure blood pressure in small mammal circulatory systems. The pressure transducer is 2F in diameter (French Scale, commonly used to designate catheter diameter; D (mm) = Fr/3), meaning it is 0.667 mm in diameter. The catheter is 0.140 m long and by inserting the probe along the channel, we could measure the pressure at any axial point along the flow path. The vibration was measured in three orthogonal axes at a point on top of the optic to examine the variance. In order to keep track of the background noise, we also checked the vertical vibration of the table where the whole system sited on. Based on the level of vibration, we used PCB 393B05 accelerometer for the optic. The frequency bandwidth we checked ranged from 0 to 1000Hz. The signals collected from those transducers were processed in Data Physics SignalCalc Mobilyzer.

Computer modeling of the system took the simplified version of the geometry and helped us to understand the dynamic situation of the experimental setup in a more general way. For transient pressure analysis, we needed use the results from experiment as an input to simulation. The model only included the simplified optic, base plate (without slots) and connecting hose (next step goal). For the complex contact of the kinematic mounting and conical washers (in the central fastener slot), we simplified those into separate springs by determining the equivalent linear spring stiffness, based on Puttock's paper [3] and the mechanical properties of the 9713K58 washers (Stainless Steel Belleville Disc Spring .190" ID, .375" OD, .015" Thick).[4] Due to the fact that ANSYS only allows the construction of points on faces, in order to add points for the definition of springs, the block and plate were divided into several parts, just as it shows in figure 5. The inside face of the flowing channel was also divided into 11 parts to apply transient pressure value for random vibration analysis. In this way, body to body springs were used to replace the sphere-cylinder and cylinder-plane contacts, easily running structural and modal analysis to figure out the mechanical force and vibration frequency. The foam under the plate could also be simulated as springs.

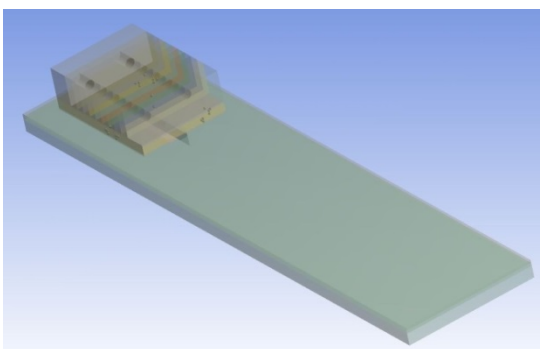

Figure 5: The simplified version of computer modeling geometry with faces divided for analyses

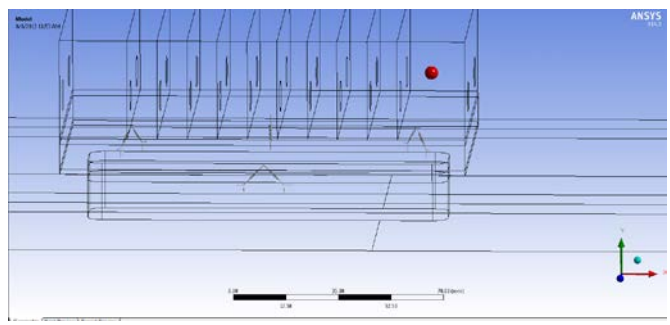

Figure 6: A close look at the springs added in geometry

Measurement results:

Note: all the result points take averages of at least 50 data points

The flow direction and port number is set up as below; when "the distance away from the end of the plate" is referred in the paper, it represents the distance from the tested position to the left end of the plate in the following chart:

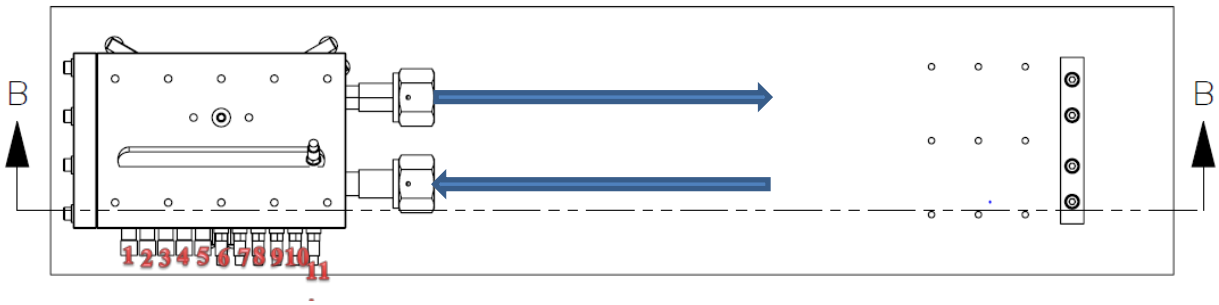

Figure 7: the scheme shows port position and flow direction

- Measurement values from PCB transducers and catheter

In order to make sure whether the pressure values obtained from 2 methods are comparable, we made measurements at 97mm away from the end of the plate (port 8) by using both Piezo transducers and catheter. The RMS and pressure spectra results are showing below in figure 8 & 9:

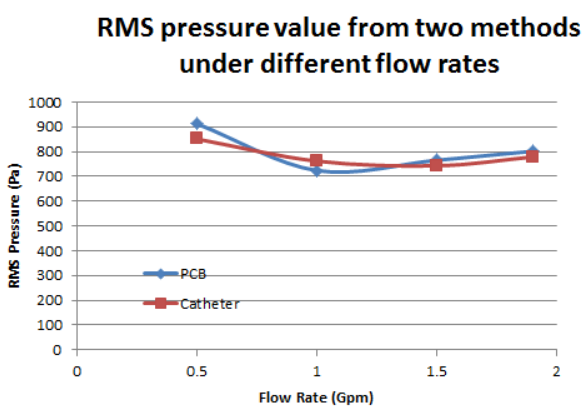

Figure 8: RMS pressure value obtained from 2 ways under different flow rates

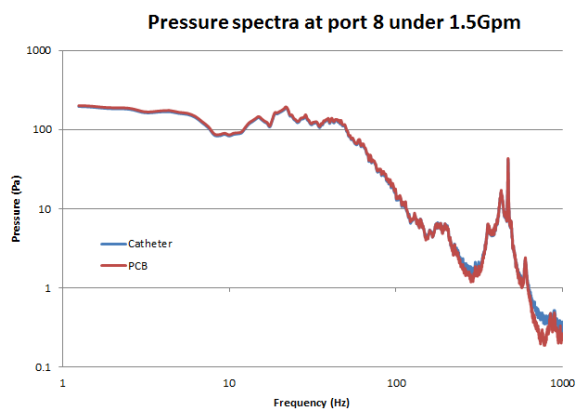

Figure 9: Pressure spectra at port 8 under 1.5 Gpm from 2 methods (log-log scale)

The values obtained from the Piezo transducer and catheter basically match with each other. One factor that can contribute to the small difference is the location within the flow. Considering the fact that because of the effect of gravity, the probe of catheter is closer to the bottom of the channel [5] which is not on the side where the Piezo transducers are located. Another factor can be the principle of the transducer operation. One thing to notice in figure 9 is that throughout the measurements, catheter always showed a higher floor noise for high frequency pressure (>800Hz) measurements and the most difference between those two methods happened there. However, the difference of RMS value is ususally less than 50Pa, which is a fairly small value in the circumstance of our experiment and the catheter has the advantage of being easily positioned anywhere along the flow path. Therefore, having verified the performance of the catheter, it was chosen as the primary measurement method.

- RMS vibration as a function of flow rate

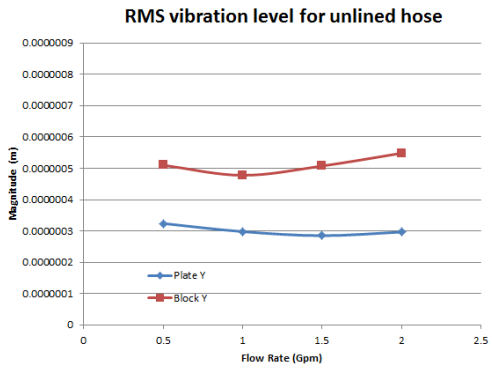

Figure 10: RMS vibration value for verticle directions of both table and optic (unlined hose)

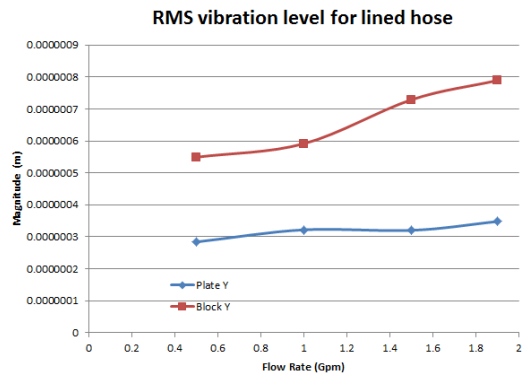

Figure 11: RMS vibration value for verticle directions of both table and optic (lined hose)

For both hoses, the overall vibration level of the dummy optic is higher than that of the plate it sits on. That is because the mounting is equivalent to several springs. As the flow drives the vibration of the optic, it is predicable that the block experiences a larger instability than the plate does. The overall trend shows here in our situation as the flow rate goes up, the vibration level of the block goes up as well. Although if we compare the RMS vibration of lined hose and unlined hose directly, lined hose did not decrease the vibration level but increase the vibration of optic instead, the variant lab background vibration might contribute to the situation. While the whole setup was installed on a vibration isolated table, the water supply hoses where found to transmit outside vibration into the structure. In the future, we need to either normalize the measurements with respect to the background level or redesign the water supply hose setup and isolate it better from the environment mechanically.

- RMS pressure as a function of axial distance and flow rate

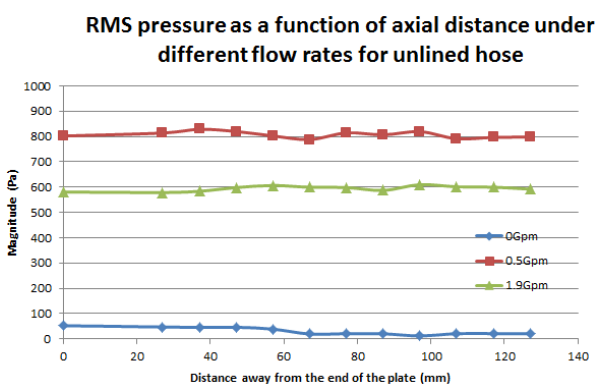

Figure 12: RMS pressure value along the optic under different flow rates for unlined hose

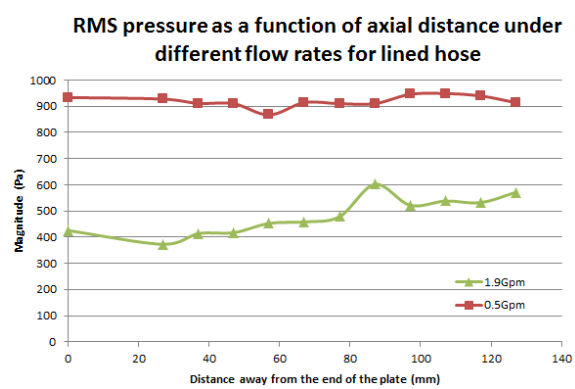

Figure 13: RMS pressure value along the optic under different flow rates for lined hose

As we can see, the pressure level along the axial direction of the flowing channel is pretty constant when flow rate is low or when unlined hose is used. For the lined hose under high

flow rate situation, it seems that pressure drop along the optic is pretty clear. An interesting thing to notice here is that when flow rate is low, the overall pressure in the channel reaches a higher value. That is because when the flow is lower, less pressure loss will happen across the hose and therefore there would be a higher pressure in the test section; In contrast, when the flow is higher, more pressure loss happens and the optic region would have a lower pressure level. Again, although RMS pressure reached a higher value when lined hose was used, it was possibly due to the change of background noise from time to time. However, the much lower value of RMS pressure for lined hose under high flow rate still proved its ability to decrease vibration.

- Pressure Spectra at different locations under low and high flow rates for lined hose

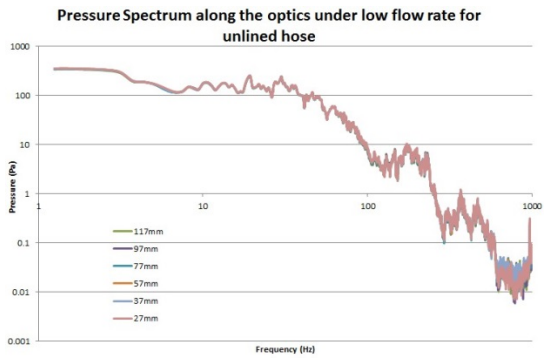

Figure 14: Pressure spectra across the optic in axial direction under low flow rate for unlined hose in log-log scale

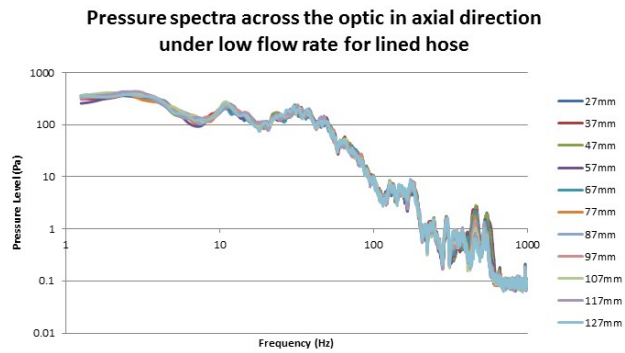

Figure 15: Pressure spectra across the optic in axial direction under low flow rate for lined hose in log-log scale

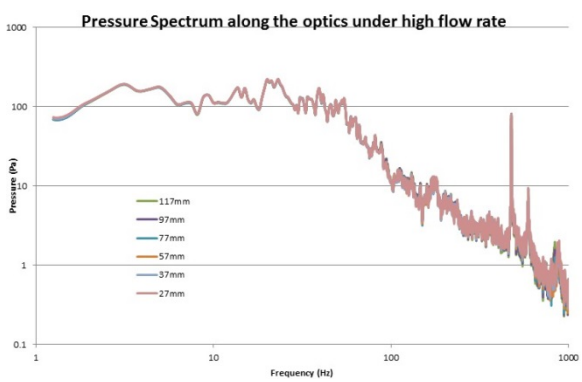

Figure 16: Pressure spectra across the optic in axial direction under high flow rate for unlined hose in log-log scale

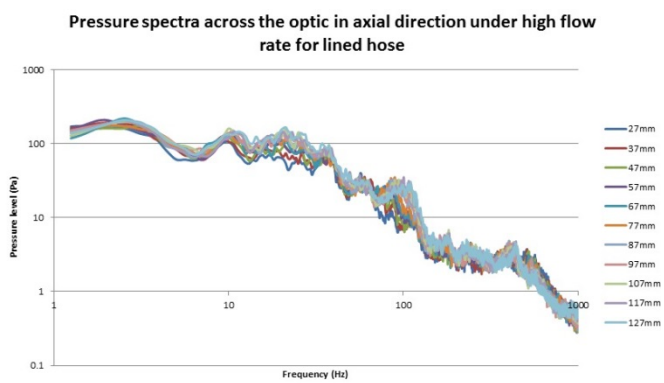

Figure 17: Pressure spectra across the optic in axial direction under high flow rate for lined hose in log-log scale

After comparison, pressure spectra at different locations had a bigger variance when flow rate was high. However, if we compare the performance of unlined hose and lined hose, we find that at low frequency range, which range we really care about vibration problem of the

optic, they have similar outputs. At high frequency, lined hose seems to be much more stable than unlined one. Therefore, we need to take a closer look at low frequency range in the future.

- Pressure spectra comparison between 2 kinds of hoses under different flow rates

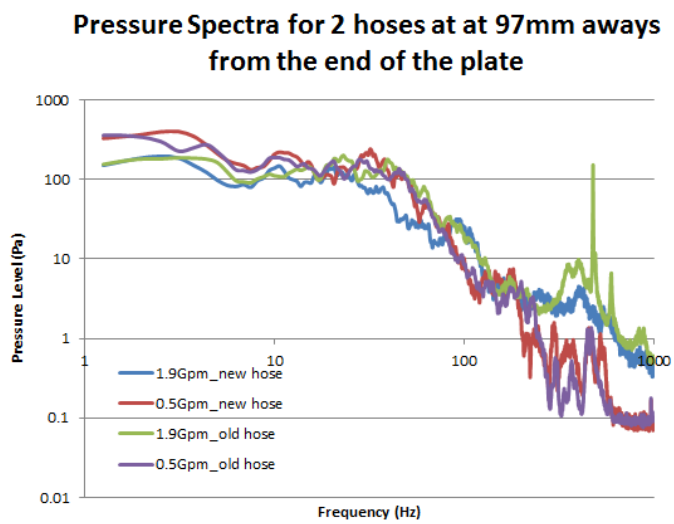

Figure 18: Pressure spectra for unlined and lined hose at the same position under low and high flow rates

For low flow rate (0.5Gpm), the unlined hose and lined hose performed similarly although peak at different frequencies. However again, throughout measurement, unlined hose spectra always had a peak at 475Hz under high flow rate, just as it shows in figure 18. From this comparison, we can see that at higher frequency, lined hose do a much better job dropping the pressure of input water thus leaving a much lower pressure level within optic channel, which can decreases the vibration level of the optic.

Simulation Process:

- Determine spring stiffness for each contact

The contacts we need to simplify consists two parts: the mounting, which includes sphere-cylinder and cylinder-plane contacts, and also the washers in the middle hole of the optic. The force-deflection relationship of mounting contact is a non-linear one [3], so if we can come up with the force on each equivalent spring system, the appropriate stiffness could be determined in those non-linear relationships. A scheme of the geometry of each mounting shows here:

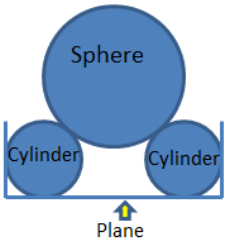

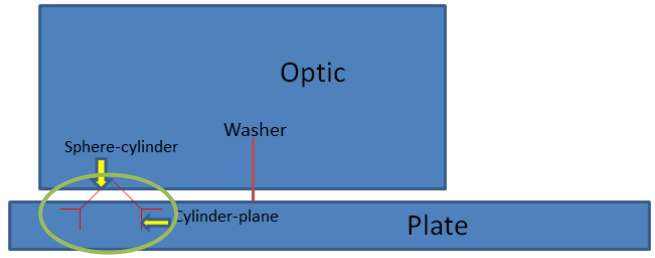

Figure 19: Real cross-section geometry of mounting contacts

Figure 20: Sketch of simplification principal

If we represent the total force applied by the washers in the middle as F, through some easy static calculation (3 mounting positions in total), we can know that each sphere-cylinder spring undergoes a force as big as 0.236F and each cylinder-plane spring undergoes a force as big as 0.167F.

Washers: According to the online information about 9713K58 washers, it deflects 0.006" with a work load of 34lbs, which is 992.4N/mm. [4] According to the formula of equivalent stiffness for spring in series,

$$\frac{1}{k_{eq}} = \frac{1}{k_1} + \frac{1}{k_2}. \tag{1}$$

And since we put 8 washers in series, the new equivalent stiffness of the system should be 124.1N/mm. As we screwed down the washer for 0.07", the total force applied on the block is about 220.6N. Therefore the force on each sphere-cylinder spring is 52.1N and that on each cylinder-plane spring is 36.8N, which values will be later used to determine the stiffness of two non-linear springs.

Sphere-cylinder contact: From Puttock's paper [3] we came up with the relationship between force and deflection:

$$\delta = 22.3635 * 10^{-5} * F^{\frac{2}{3}} \tag{2}$$

where force is in N and deflection is in mm

According to the particular force on this type of springs calculated before (52.1N), we took the derivative of this function relative to force and we got

$$\delta' = 14.909 * 10^{-5} * F^{-\frac{1}{3}} \tag{3}$$

Then once we plugged in 52.1N for F, we knew the slope of the force-deflection diagram at that particular point, which was the inverse of stiffness of that non-linear spring. Therefore after some calculation, the stiffness for sphere-cylinder contact in our situation turned out to be 25031.92N/mm.

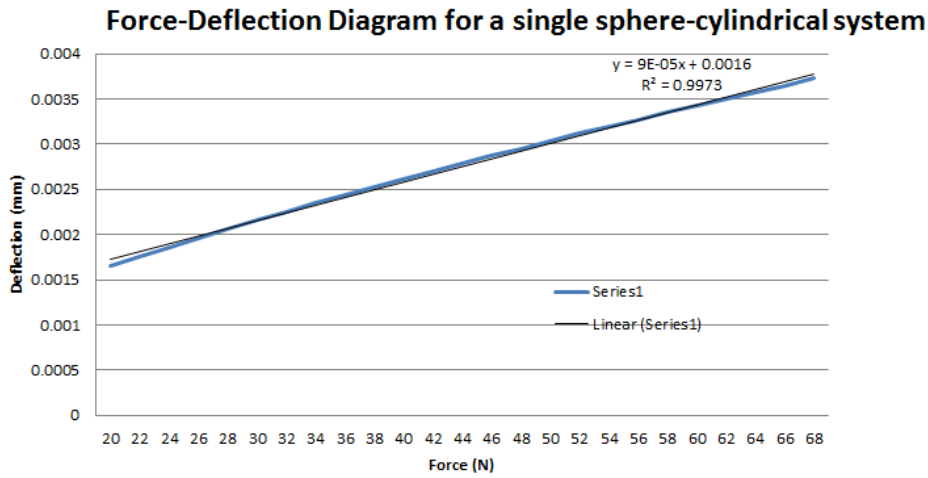

Figure 21: Force-deflection curve for a single sphere-cylinder spring

Cylinder-plane contact: Through similar process, the stiffness for this system turned out to be 719400.74 N/mm.

Foam: For the stiffness of the foam which was inserted under the plate to create a non-fixed system, we measured its original height and compare the value with its height under some known weight. After calculation, its stiffness turned out to be 59.14N/mm.

- Simulation Results

1. Structural Analysis Results

   From ANSYS structural analysis, the simulation value of force on each sphere-cylinder spring is almost the same as we expected: about 52N. However, the force on each cylinder-plane spring is a little more asymmetric than expected. Each vertical ones has a force around 6N, but each horizontal ones barely takes any pressure, usually under 1N. Although on the side of the block which only one mounts exists, the two values are closer, 3N and 4N respectively. In terms of deformation, it shows that each of the sphere-cylinder springs deflects about 2E-3mm and each of the cylinder-plane springs deflects less than a few nanometers. A picture of the total deformation is showing here:

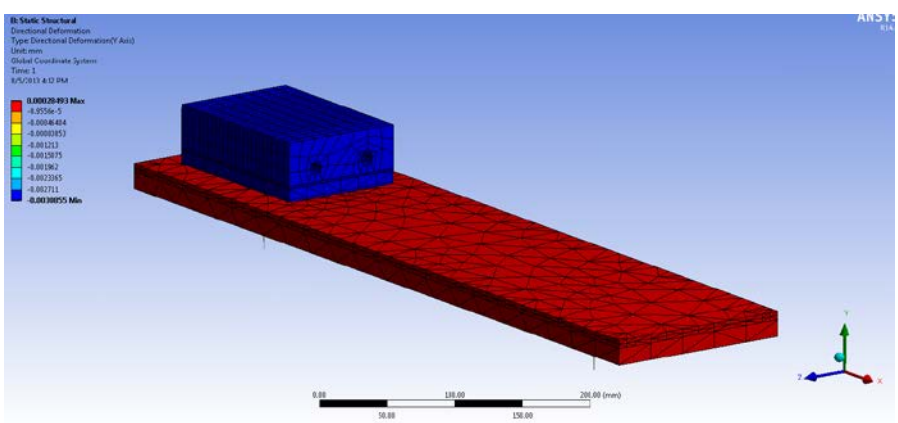

Figure 22: the diagram of total deformation in structural analysis

2. Modal Analysis Results

For modal analysis, we considered two situations: fixed and non-fixed system. The relevant results are above the first six modes because these modes are rigid body modes (6 degree of freedoms), which are really close to 0Hz. Therefore in our simulation, we checked number 7 to number 12 modes:

Boundary Condition / Mode #	Non-fixed (Hz)	Fixed (Hz)
7	252	207
8	511	425
9	546	454
10	731	651
11	823	752
12	839	795

Because the real experiment (foam underneath the base plate) is more similar to non-fixed situation, we compare the simulation results with the peak frequencies we get from impact experiments. However, even though on the pressure spectra from experiment some peak did matches, it seems that the simulation missed a lot of other peaks.

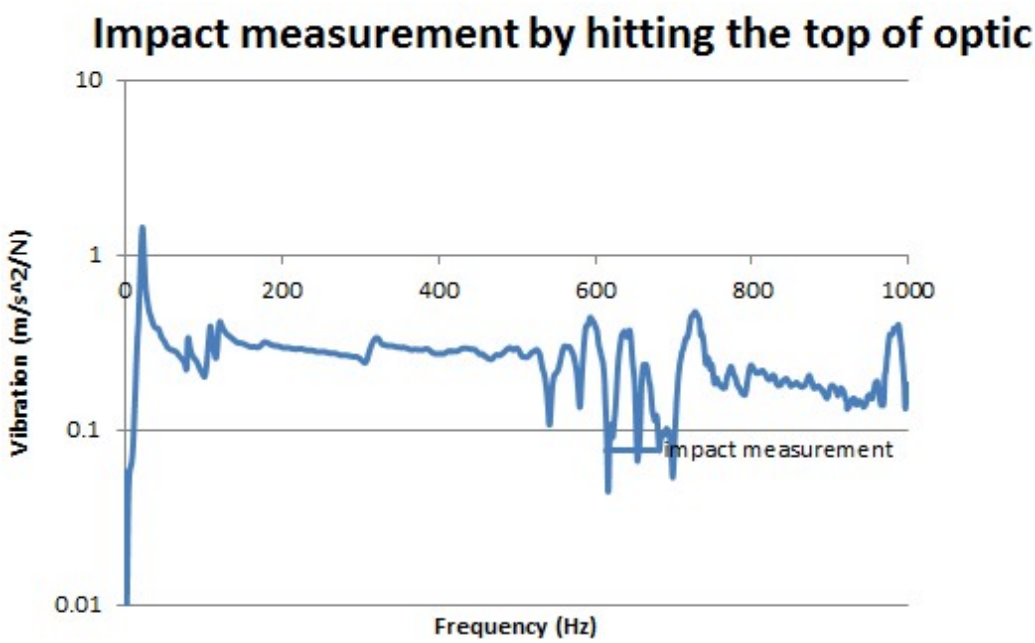

Figure 23: Experimental vibration spectra for the setup

An important reason why experiment and simulation results did not match in modal analysis is due to unmodeled portions of our system, especially the hose. The geometry effect of the hose in experiments definitely contributed to some peaks in pressure spectra. The following plots show the mode 7 vibration for both fixed and non-fixed situation.

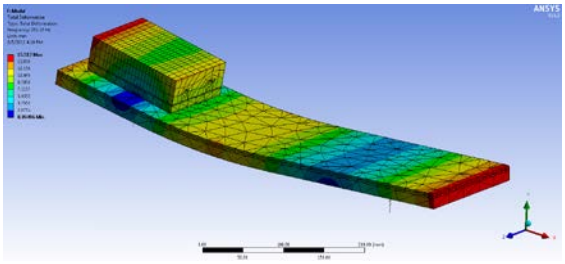

Figure 24. Mode 7(plate deformation) for non-fixed system

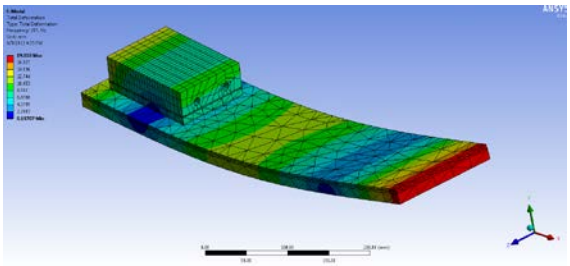

Figure 25. Mode 7(plate deformation) for fixed system

3. Transient pressure analysis
   In transient pressure analysis, we used pressure data we got from experiments as input to out simulation. We divided the internal channel in optic into 11 parts and applied the time variant pressure values on the channel wall. Right now, we only made a sample run by applying pressure on only 1 part of the channel wall and it works. The next step is to apply all data points and compare the vibration spectrum we get from simulation with that from experiment.

Conclusion:

In this project, we investigate flow-induced vibration of our optics model and run some computer simulations. We find that generally the vibration level is related to the flow rate: higher the flow rate, larger the vibration level. For the SPR-320 pressure catheter from Millar Instruments, it performs not correctly under high frequency (> 800 Hz). Although we did not find a lot of interesting difference of vibration level in low frequency range between the two hoses, the lined hose turns out to have a smaller pressure fluctuation under high flow rate in pretty high frequency (about 475Hz), which should correlate to lower vibrations and we hope to investigate this further. Also, the simulation is working and matches the real experiment in some extent, but we need further develop it and use it to understand the dynamics of X-ray optics more.

Future Work:

- More measurements to check background variance, then either normalize background in results or redesign the setup to make it more mechanically isolated
- Finish ANSYS transient pressure analysis using all the data points and compare the vibration situation results with experiment results
- Simulate the hose into system and run analysis again

Acknowledgements:

This project runs under Advanced Photon Source Engineering Support group (AES) in Argonne National Laboratory. I am really grateful to my mentors Curt Preissner and Jeff Collins. They are extremely patient and helpful during this internship. I would also like to thank Jie Liu and Branislav Brajuskovic for simulation tech help. Thanks to Karen Davis and Loretta Cokeley for

making my internship ran smoothly. Finally, I want to extend my thanks to Linda Spentzouris and Eric Prebys and other people who helped organize Lee Teng research internship and make it such an unparalleled opportunity.

References:

[1] M. J. Laughlin, "Mirror jitter: an overview of theoretical and experimental work," Optical Engineering, vol. 34, pp. 321-329, 1995.

[2] R. J. Tobin & I-Dee Chang, “Wall Pressure Spectra Scaling Downstream of Stenoses in Steady Tube Flow,” J. Biomechanics, vol. 9, pp. 633-640, 1976

[3] M .J. Puttock & E. G. Thwaite, “Elastic Compression of Spheres and Cylinders at Point and Line Contact,” National Standards Laboratory Technical Paper No.25, Commonwealth Science and Industrial Research Organization, Australia, Melbourne 1969

[4] McMaster-Carr, http://www.mcmaster.com/#catalog/119/1228/=nmw56x

[5] Y. Yazicioglu, T. J. Royston, T. Spohnholtz, B. Martin, F. Loth, and H. S. Bassiouny, "Acoustic radiation from a fluid-filled, subsurface vascular tube with internal turbulent flow due to a constriction," Journal of the Acoustical Society of America, vol. 118, pp. 1193-1209, 2005.